

JPMTR 127 | 1820
DOI 10.14622/JPMTR-1820
UDC 676.2:547.4/667.6

Research paper
Received: 2018-12-06
Accepted: 2019-09-05

The starch addition to a curtain coating formulation and its effect on pitting

Samantha L. Schoenfelder, Alexandra Pekarovicova and Paul D. Fleming

Center for Printing and Coating Research,
Western Michigan University,
4601 Campus Drive, A-217 Floyd Hall, Kalamazoo, MI 49008

a.pekarovicova@wmich.edu

Abstract

An undisclosed recycled fiber board mill installed a “two-slotted” curtain coater to replace an air knife coater, which enabled a high-quality coating without past speed limitations. With the curtain coater’s installation, however, a prominent defect arose, known as “pitting”. Pitting occurs when the coating of the sheet has small holes that mar its surface, which, when clustered together or larger in size, can cause print break-up. Starch was added to the formulation to modify rheological properties of top and bottom curtain coatings, and advance water retention capabilities of them. Results show the original formulations with no starch were more thixotropic than the starch formulations. Starch aided in reducing the low shear viscosity by as much as 25 %, which had a large impact on converting the system from a strongly elastic rheology to a more viscous one. Such a move toward a more purely viscous system helped to prevent the elastic stretching and reduced bubble formation in the coatings. Starch addition also increased water retention capabilities of the coatings. The pitting significantly decreased during these trials, with lower overall pit counts and area pitted.

Keywords: coating color, coated paperboard, air entrapment, rheology, surface free energy

1. Introduction and background

The utilization of recycled paperboard within the packaging industry creates a competitive need to continuously improve production by finding advancements to create a superior product in a timely and cost-effective manner. These engineering advancements assist in manipulating production, while maintaining quality and trialing new applications to promote the highest optimization for the paper machine. Changes can be made at all parts of the process, from source of fiber over the coating, to actual machinery installations as new modifications are developed. It is an ever changing, developing industry, which does not have the option for complacency.

Curtain coating is currently a more and more chosen method for single or multiple coating layer applications for high speed coating of various coat weights, ensuring smaller pores than obtained with other coating methods, leading to better print quality (Birkert, et al., 2006). Curtain liquid coating is falling freely, with gravity accelerating the falling curtain, until it falls

on the moving substrate (Becerra and Carvalho, 2011; Liu, et al., 2016). Certain operating parameters need to be held in the “coating window”, otherwise various defects may occur. High speed of web compared to curtain velocity causes bead pulling forward, but on the other hand, slow web movement compared to curtain velocity causes its upstream movement, so called heel formation. Air entrainment underneath of liquid bead may be caused by too high web speeds and lastly, the curtain may break into columns at its very low flow rate (Becerra and Carvalho, 2011).

A single curtain coating layer employs a curtain slot die as well as a curtain slide die. For multiple film applications, curtain slide dies are mostly used. Curtain coating is becoming popular in cardboard grades for packaging (Döll, 2010). One of the drawbacks of the process is the air entrainment, creating bubbles in the coating. Air entrainment has been cited as the leading cause of pitting (Figure 1) in theoretical and experimental capacities, occurring between substrate and impinging coating, because of interfacial tension constraints (Urscheler, et al., 2005).



Figure 1: SEM image of pitted surface of curtain coated board

The air film is unstable and breaks into bubbles, creating visible defects (pits/craters) that are usually related to the curtain's coating interface in contact with the base coat that is in contact with the substrate (Urscheler, et al., 2005). Most curtain coaters have a vacuum device installed near the impingement zone, which acts as a deaerator, but these do not always have the capacity to remove all the boundary air that can cause entrainment and lead to pitting. Therefore, as web speeds increase, the removal of boundary layer air becomes progressively more difficult by the vacuum and manifests itself as the onset of air-entrapment in the impingement zone (Tripathi, 2005; Tripathi, et al., 2009). For very high web speeds, steam substitution (Tripathi, 2005; Tripathi, et al., 2009), where saturated steam is injected before the impingement zone to remove boundary layer air, may be applied. Furthermore, roughness of a substrate and poor wettability may lead to a higher amount of air entrainment. Without a direct metering device, the substrate does not require special strength properties for good runnability (Renvall, et. al., 2013), but a curtain will follow the contour of low/high amplitude roughness. With a high frequency of varying roughness, the coating film becomes more complex and sometimes incapable of keeping its form, where high base sheet roughness may create craters (Figure 2) (Tripathi, 2005).

Both figures (Figure 1 and Figure 2) show visible pits on the top coated layer. Air entrainment is also synonymous with dynamic wetting failure, with critical parameters being speed and viscosity (Becerra and Carvalho, 2011; Liu, et al., 2016), but also found to be dependent on surface tension (Marston, et al., 2009). In order to fully understand wetting, one must look at viscosity and surface tension as tools to combat the effects of high speeds and lower the possibility of air entrapment. In the case of high speed curtain coater equipped with saturated steam, the environment is

defined by the temperature of steam used to eliminate air at the interface. This raised temperature of the coating leads to a rapid and significant drop in viscosity of the coating, especially a decrease in the viscoelasticity. However, the dual slotted curtain coater discussed here does not facilitate steam substitution, since it is totally enclosed, although has temperature and air relative humidity control (21–24 °C, 50 % RH). Thus, other solutions must be sought to control pitting.

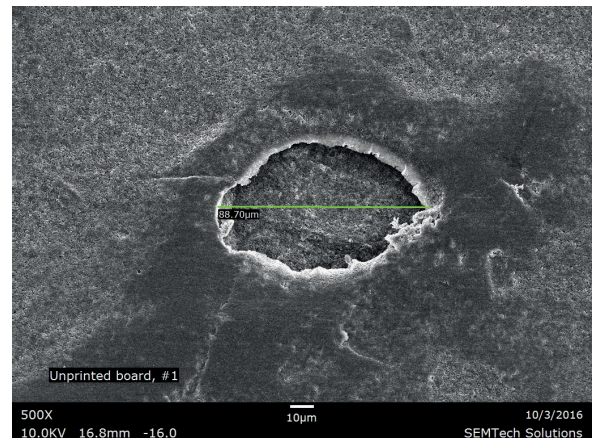


Figure 2: SEM image of large pit on curtain coated board

Curtain coating suspensions are known to be pseudo-plastic, which means that they are shear-thinning, or their viscosities decrease as the shear rate increases. It has been suggested that rheological properties of the coating are critical to avoid or reduce the presence of pitting, because they influence how easily air bubbles can be extracted from the coating color (Tripathi, 2005; Triantafillopoulos, et al., 2004; Kistler, 1983).

Thus, in order to deter air entrainment, the promotion of wetting through rheological properties is critical at impingement as it affects the process in multiple ways. As the liquid coating displaces gas at a dynamic wetting line (when the coating meets the web), it will create a continuous film of coating that is deposited on the moving substrate (Kistler, 1983). Close to the respective wetting lines, there are comparatively short regions of rapidly rearranging shear and extensional flow, which is even more complicated with non-Newtonian fluid-like coating (Kistler, 1983). Low coating viscosity can cause a splash to occur at the web, while extensional viscosity is the key to preventing heel forming (Tripathi, 2005; Chen, et al., 2016), both highly affecting the amount of air that will be dragged under the film. Thus, rheological properties of the coating are critical to avoid or reduce the presence of pitting, because they influence how easily air bubbles can be extracted from the coating color (Tripathi, 2005). As previously stated, the air entrainment will then form bubbles, which lead

to pitting. Curtain stability cannot only be improved with a thicker curtain, greater curtain velocity, and higher volumetric flow rate per unit width, but also with a lower coating surface tension (Brown, 1961).

Thus, surface tension is an important component of a coating, particularly at slow speed. It was also found through experimentation that the air entrainment phenomenon is strongly dependent on surface tension, a fact already well established for various other coating methods (Marston, et al., 2009; Klass, 2004). Lowering surface tension can result in higher viscous drag on the curtain, increasing the radius of curvature of the pulled film over the impingement zone, and reducing total pressure, resulting in delayed and reduced air entrainment (Tripathi, et al., 2009). Without proper wettability, air entrainment is promoted between the coating and the substrate, and the coating will literally not adhere to the substrate (Chen, 1992; Pekarovicova and Fleming III, 2005; BASF, 2016). The aim of this work was to focus on a coating (and board) related defect known as, “pitting” or “pinholes,” which causes an abnormal surface of the board that will not print smoothly. This issue was occurring at a recycled board plant, which has been troubleshooting it since their air knife coater was replaced by a curtain coater. In this work, coating formulations were altered to fight pitting.

2. Materials and methods

2.1 Procedures

Experiments were done on a Fourdrinier paper machine, using 100 % recycled fiber material to produce a three-ply paperboard, running at 460–610 m/min (1500–2000 fpm). The three plies consisted of a top liner, filler, and back liner, with caliper of 0.457 mm (18 mills or 18 pt). The board was first bar precoated, and then submitted to high speed two slotted curtain coating, done wet-on-wet at ambient temperature. The original curtain coater formulations for the top and base curtain coatings are found in the Table 1.

Table 1: The DF base and top coatings original basic formulation (pph – parts per hundred parts of pigment)

Materials	DF base original basic formulation (pph)	DF top original basic formulation (pph)
Clay	100.00	90.00
TiO ₂	0.00	10.00
Latex	21.00	21.00
Thickener	0.35	0.35
Dispersant	0.12	0.12
Surfactant	0.30	0.30

The addition of 3 parts of a dry starch product per hundred parts of pigment (pph) to the base and top direct fountain (DF) coatings was made to see the effects on pitting (Table 2). The trial samples rheology, Brookfield viscosity, high-shear viscosity, and water retention value (WRV) were tested and compared to the control (original formula) formulation’s measurements. Starch origin, molecular weight and its properties were proprietary, and thus they cannot be revealed. However, it was expected that starch exhibits a typical proportion of amylose and amylopectin.

Table 2: Formulation of DF base and top coating for trial with added starch (pph – parts per hundred parts of pigment)

Materials	DF base starch trial (pph)	DF top starch trial (pph)
Clay	100.00	90.00
TiO ₂	0.00	10.00
Latex	21.00	21.00
Thickener	0.25	0.25
Dispersant	0.12	0.12
Surfactant	0.30	0.30
Starch	3.00	3.00

The modified DF base coating formulation (Table 2) first had 0.35 pph of thickener and 2 pph of starch, which increased Brookfield viscosity from ~400 mPa·s to ~600–700 mPa·s at a shear rate of 26.3 s⁻¹ and it was seen as an operational concern to the mill. It is above target for the suggested Brookfield viscosity, and it started to cause physical build-up in the system. To ensure long-term success, it was decided to lower the thickener from 0.35 pph to 0.25 pph, and increase the starch from 2 pph to 3 pph. This brought the viscosity down to ~300–350 mPa·s.

Viscosity (in mPa·s) of the coatings was measured by a Brookfield DV-E viscometer at 100 RPM with the (RV) spindle #3 at a shear rate of 26.3 s⁻¹ at 25 °C. The high shear viscosity was measured on a Hercules DV-10 viscometer with an E-Bob. The averages of three measurements of a ramp up from 0 s⁻¹ to 46288 s⁻¹ shear rate (0–4 400 RPM) back down to 0 s⁻¹ (0 RPM) per coating at 25 °C were recorded.

The WRV determinations were done on coated samples that were taken from the paper machine and tested by the AA-GWR Water Retention Meter (model 250) by Kaltec Scientific, Inc. according to TAPPI Standard T-701 pm-01 (TAPPI, 2005). Solids content was measured using an IR heated balance until constant sample weight was achieved. Instrument software calculated solids content automatically. Density of the wet coating was determined gravimetrically using weight per gallon stainless steel cups.

2.2 Pitting tests

A pitted sample was stained with a Croda manufactured red drawdown ink (MBR 10039) to better see the pitting on the sheet. This also makes it easier for the image analysis software to read. There are three numbers that help determine the amount of pitting on the sheet: large pit count, proportion of pitted area (in %), and overall number of pits per measured area, which was 6 mm × 6 mm.

Each trial assessment requires a paper tester to look at four random and separate areas of the sheet in the cross-machine (CD) direction. The large pit count is taken with a Barska brand handheld digital microscope (AY11336), with a 10–300 × magnification, which is placed on the stained sheet. The higher magnification, but lower resolution highlights larger pits, and dulls out the smaller pits, showing only large pits are in the visual area of interest (greater than 1 mm in diameter). The paper tester rates the sample on a scale of 1–4. Thus, after four tests, the lowest pit count is ranked 4 and the highest is 16. According to claims filed against the mill, printing issues tend to occur when the large pit count reaches ranking of about an 8. There is obviously variability in data due to the dependency on human perception and opinion. The proportion of pitted area and number of pits were both found through the use of a 200 × magnification Aven brand digital microscopic camera (Mighty Scope NIR 5M). A public domain software, ImageJ, was used to analyze these images, which is able to distinguish pits through the contrast of color (pits are darker red, filled in by the Croda ink). It digitally computes the average proportion of pitted area and number of pits through the four measurements.

3. Results and discussion

Through SEM images (Figures 3 and 4), it's easy to see the differences in depth and width of the pits and caves, which range from smaller pinhole-like sizes, to larger crater-like that are 80 μm wide or larger, both of which can be up to over 20 μm deep. Figure 3 clearly shows a pit crater on the top coating layer, whereas in Figure 4 can be seen caves in one or the other DF coated layers or possibly in between the two. Through experimentation and research, causes of pitting have been narrowed down to a few mechanisms: air entrapment, wetting of the substrate (governed by physical and chemical behaviors such as coating properties), and substrate roughness (Lee, et al., 2009). All three are interconnected, and can be addressed by certain coating properties. Moisture within the sheet was also suspected, but through multiple trials deemed a less critical mechanism at this point; varying drying tem-

peratures were tried twice and found inconclusive, and without a statistical effect on pitting. Challenges faced within the paperboard industry have been the need to develop the right formulations to operate at higher flow rates, higher solids, higher curtain heights, and high web speeds compared to the photographic and specialty paper applications (Tripathi, 2005). Thus, in order to successfully know how to combat pitting, it is useful to understand what exacerbates the defect, and how the coating formulation can be manipulated to reduce it.

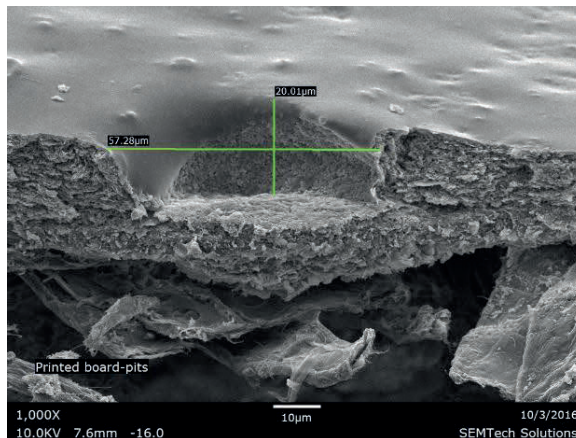


Figure 3: SEM cross-section image of a pit

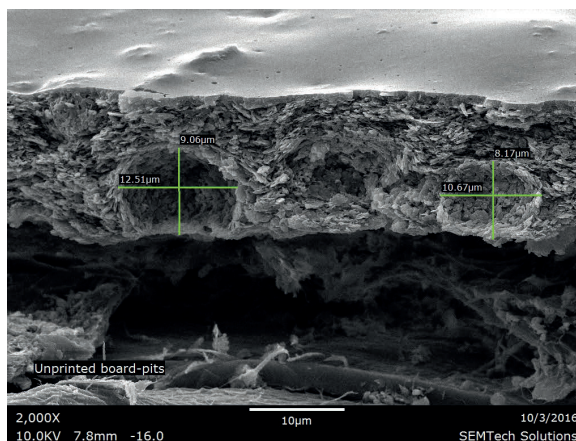


Figure 4: SEM image of cross-section cave pitting / air entrapment under the surface

The original DF top and base coating formulations can be seen in Table 1. A brief analysis of the board was performed in order to better understand the surface on which the coating is applied (Table 3). It is known that pitting only occurs when the rod precoat and the curtain coatings are all applied and does not occur when only the precoat or the curtain coatings are applied. Thus, a comparison of the coated paperboard and the precoated paperboard was completed to see any similarities and/or differences that might reveal any indications behind the pitting phenomena.

Table 3: Uncoated vs. precoated paperboard – summary of paper properties, average (AVG) and standard deviations (STD), from Schoenfelder (2017)

Test		Uncoated paperboard	Precoated paperboard
Surface free energy (mJ/m ²)		70.7	46.6
Dispersive component (mJ/m ²)		31.1	43.9
Polar component (mJ/m ²)		39.6	3.7
Porosity – Gurley (s/100 cm ³)	AVG	48.0	850.0
	STD	6.0	107.0
Roughness – PPS (µm)	AVG	6.6	4.5
	STD	0.4	0.3
Roughness – Sheffield Units (SU)	AVG	304.0	260.0
	STD	8.0	26.0

Three major properties of the board were of interest: surface free energy, smoothness/roughness, and porosity. Surface free energy (mJ/m²) of the board will help to quantify the interactions between the surface and the liquid coating (surface tension), and therefore provides an insight into the wetting of the paperboard at the dynamic wetting line. Smoothness or roughness is of importance since it was noted in the Introduction that a rougher sheet could allow for more boundary air entrainment. Porosity (more correctly permeability) is of interest, since a greater porosity will allow for more wetting, where the coating will tend to dive into the sheet; this could also allow air and moisture to escape through more passages, where a less porous sheet will force air and moisture through the top of the coating. The averages of ten individual readings of all properties (besides surface free energy, which was calculated using various contact angle measurements and the Owens and Wendt (1969) method), were calculated and are summarized in Table 3. The surface free energy of the uncoated board is considerably higher than the precoated board (Table 3), which will result in faster, more complete wetting of a liquid on the surface. This value is probably skewed, due to the high porosity of the sheet, which will contribute to the wetting of the surface and produce a false surface free energy value; a Cobb test confirmed this theory, as there was complete wetting in less than 1–2 seconds on the uncoated surface.

The DF top and base coating formulations were modified by adding 2 pph of dry starch to an ~3.6 t (8000 lb.) batch of each coating (Table 4). Otherwise, the coating formulations stayed the same. Static surface tension of both coatings was measured. For starch coating, its value was slightly higher than that of original (control) one (Figure 5).

The DF base starch formulation would run first, in order to ensure curtain stability and machine runnability. If the run was smooth, the operators would then

transition the starch into the DF top slot as well. It was planned to run on 0.457 mm (18 pt) board, but due to the unpredictability of machine runs and customer demands, the trial was run on 0.356 mm (14 pt) board.

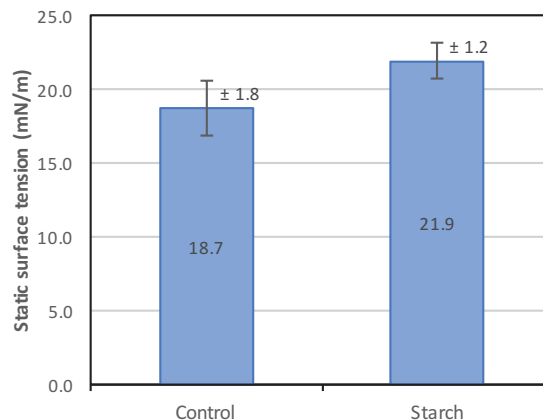


Figure 5: Static surface tension (SFT) for control coating vs. starch coating

Later, also other calipers were tested. Long-term results (Schoenfelder, 2017) of pitting on different caliper boards are given in Table 4. The average proportion of pitted area showed a significant decrease from 4.1 % to 2.6 % (Table 5), with each caliper showing a substantial drop in area, besides 0.558 mm (22 pt), which stayed virtually the same. There is also less variability in pitting, with lower standard deviations, which means there is more predictability in the product outcome through the use of starch.

Coating samples were taken at the DF curtain head, and WRV were monitored to better indicate when the starch was fully integrated into the system (the WRV value was expected to decrease with the addition of starch).

Pit counts immediately dropped from 8 to 5 when the DF base trial coating reached the DF head; proportion of pitted area decreased from 5.8 % to 3.6 %. This decrease in pitting was consistent within the duration of the trial, with the overall large pit counts decreasing to an average of 4.1 % and pitted area decreasing to 2.6 % after both DF base and top trial coating batches reached the DF head. Pre-trial pitting is illustrated at the Figure 6 and the decrease in pitting after starch addition is shown in Figure 7.

The coating rheology could be manipulated by the addition of starch to promote further healing properties and increase water retention capabilities.

It is possible that the amylose starch linear structures with no side chains in the starch mixture are responsible for such behavior, where it's also known to be

Table 4: Longterm average (AVG) and standard deviations (STD) data of caliper vs. pitting for starch added in DF base (Schoenfelder, 2017)

Grade / Caliper	Large pit count		Proportion of pitted area (%)		Number of pits	
	AVG	STD	AVG	STD	AVG	STD
0.356 mm (14 pt)	4	1	3.1	1.2	4958	1941
0.406 mm (16 pt)	5	1	2.8	1.2	4608	2062
0.457 mm (18 pt)	4	0	2.6	1.2	4434	1915
0.508 mm (20 pt)	4	0	2.4	1.0	4236	2131
0.533 mm (21 pt)	4	0	2.6	0.7	4730	1395
0.558 mm (22 pt)	4	0	3.7	1.3	6487	2255
Overall AVG	4	1	2.6	1.1	4521	2033

Table 5: Starch trial summary – pitting averages (AVG) and standard deviations (STD) viewed from an area of 6 mm × 6 mm

	Large pit count		Proportion of pitted area (%)		Number of pits	
	AVG	STD	AVG	STD	AVG	STD
Control / pre-trial	7	1	4.1	0.9	5300	1100
Trial – starch	4	1	2.6	0.8	2900	310

hydrophilic in nature. Vinyl acrylic latex may have side chains or copolymers in their chain, with unknown amounts of -COOH groups, and side branches of various amounts and sizes, all of which may affect packing of polymer molecules in the coating and thus affect viscosity. The original formulation (control) and the

starch trial formulation (with the decreased thickener component) were both tested for the following basic coating properties: surface tension (Figure 5), density (Figure 8), solids content (Figure 9), Brookfield viscosity (Figure 10), high shear viscosity vs. shear rate (Figure 11), and water retention values (Figure 12).

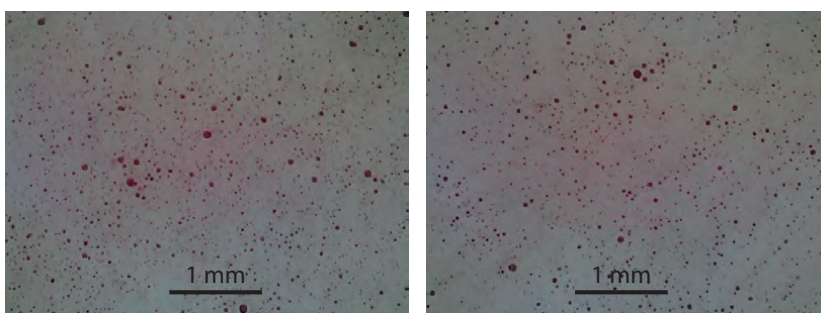


Figure 6: Pre-trial (control) sample images

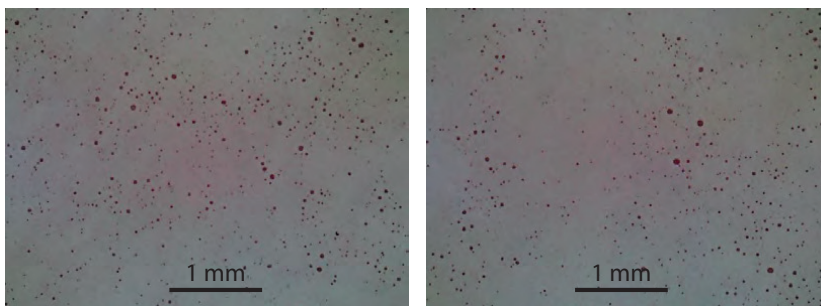


Figure 7: Trial starch sample images

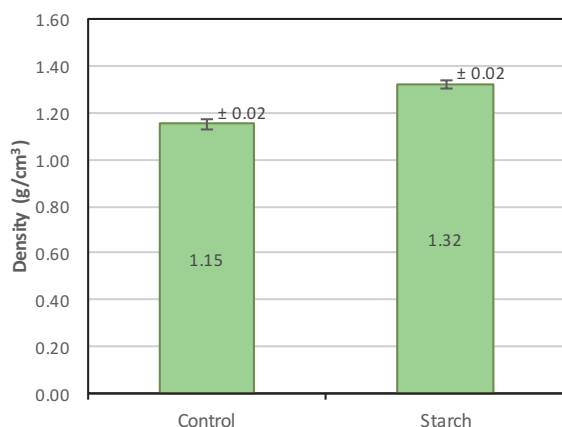


Figure 8: Density of control coating vs. starch coating, adapted from Schoenfelder (2017)

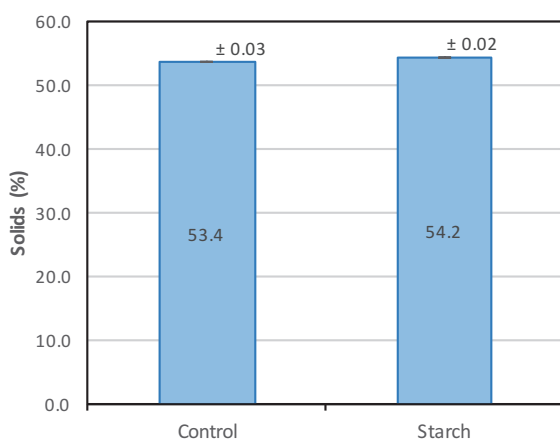


Figure 9: Solids of control coating vs. starch coating, adapted from Schoenfelder (2017)

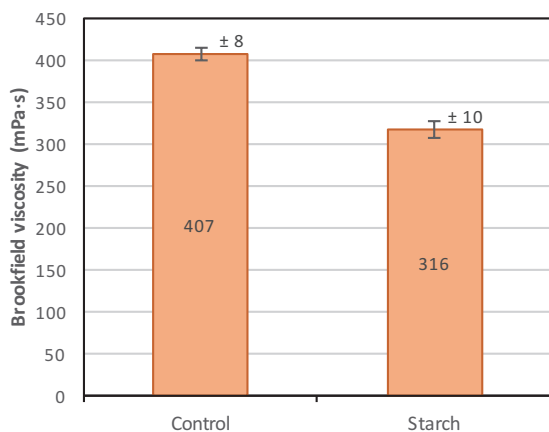


Figure 10: Brookfield viscosity of control coating vs. starch coating at 26.3 s⁻¹ shear rate

Through these results, one can see that the starch allowed for slightly higher solids (in %) and a higher density (in g/cm³) of the coating, but it's Brookfield

viscosity (at 26.3 s⁻¹ shear rate) was considerably lower than the original formula of control sample (Figure 10).

This might be attributed to the decreased thickener content, which may have increased viscosity (per part) more than the starch is capable of. The pH values of the coatings are not considerably different (data not shown, Schoenfelder, 2017), with the starch being slightly closer to neutrality than the control sample formula. This will not change the effect of the coating performance on the machine.

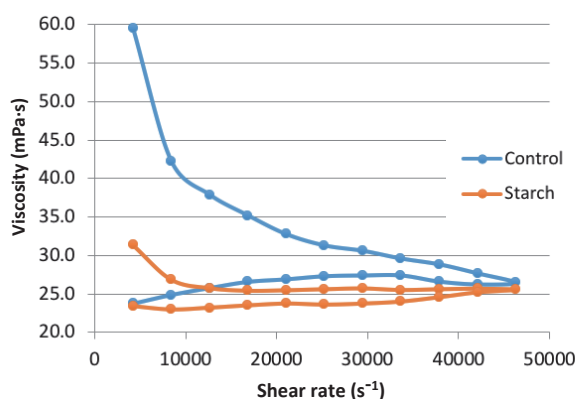


Figure 11: High shear viscosity vs. shear rate of the control coating and starch coating (Schoenfelder, 2017)

While both coatings show a pseudoplastic (shear-thinning) model curve, the control formulation has a higher initial viscosity (Figure 10), which quickly declines (Figure 11). This gives the control coating a larger area between the ramp up and the ramp down sections of the test; the area between the initial ramp up from 0 s⁻¹ to 46288 s⁻¹ and the final ramp back down to 0 s⁻¹ can help define how thixotropic a coating is – the larger the area the more thixotropic or shear thinning it obviously is (increased drop of viscosity). Thus, the control formulation is more thixotropic than the starch formulation. Low shear viscosity of coating colors usually reflects the viscoelastic region. Reducing the low shear viscosity by as much as 25 % has a large impact on converting the system from a strongly elastic rheology to a more viscous one. Such a move toward a more purely viscous system is known to prevent the elastic stretching and visible retention of coating color defects, such as bubbles.

The WRV measures how much water is released by a coating after drying. In theory, if water is held in by the coating instead of being released by drainage, there is a lower probability of the water creating air/vapor and bursting through the curtain coating layers during the drying process. Starch is hydrophilic in nature, and thus it is believed that the gravimetric WRV of the coating will decrease, as the coating will be able to hold on to more water.

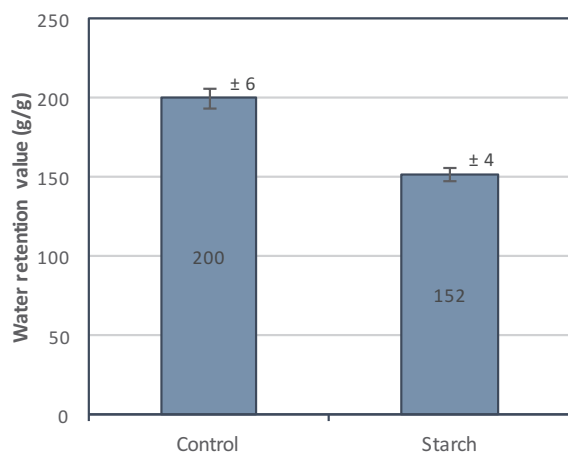


Figure 12: Water retention value (WRV) of control coating vs. starch coating (Schoenfelder, 2017)

Figure 12 shows the WRV results of the test on the control vs. the starch trial formulation. The results show improved water retention capabilities of the coating through the introduction of starch. It was found through lab trials that an increase of the starch content

within the coating batch did not help to lower the WRV any further, thus 150 g/g WRV seems to be where the starch's capabilities plateau. This significant drop from 200 g/g to 150 g/g WRV may help to decrease pitting, with water being held in the sheet and/or coating, not released through the coating. This also suggests that the formulation is less flocculated, and thus also less elastic.

4. Conclusion

The addition of starch to base and top coatings showed beneficial effects on decreased pitting area and size of pits. Addition of starch paired with decrease in the thickener addition resulted in decreased viscosity of the curtain coating. The viscosity was still around/above the 300 mPa·s range. Water retention levels of coatings seem to correlate with lower pitting – as the coating holds in more water, there is most likely less air passing through, which may be a mechanism for pit formation. The roughness of the base sheet (Table 3) might be adding to the overall pitting issue. The surface tension of the coating promoted increased wetting capabilities, but this did not affect pitting.

References

- BASF, 2016. *Surface Control*. [online] Available at: <https://www.dispersions-pigments.basf.com/portal/basf/ien/dt.jsp?setCursor=1_564555> [Accessed 8 May 2018].
- Becerra, M., and Carvalho, M.S., 2011. Stability of viscoelastic liquid curtain. *Chemical Engineering and Processing: Process Intensification*, 50(5–6), pp. 445–449. <https://doi.org/10.1016/j.cep.2010.11.011>.
- Birkert, O., Hamers, C., Krumbacher, E., Schachtl, M., Gane, P.A.C., Gerteiser, N., Ridgway, C.J., Fröhlich, U. and Tietz, M., 2006. Curtain coating of pigment coats. *Professional Papermaking*, 2, pp. 56–71.
- Brown, D.R., 1961. A study of the behavior of a thin sheet of moving liquid. *Journal of Fluid Mechanics*, 10(2), pp. 297–305. <https://doi.org/10.1017/S002211206100024X>.
- Chen, K.S., 1992. *Studies of multilayer slide coating and related processes*. PhD thesis. University of Minnesota.
- Chen, T., Joyce, M.K., Fleming, P.D., Lee, D.I. and Bloembergen, S., 2016. Pigmented formulations containing biobased nanoparticle binders for curtain coating applications; Part 1: Rheological study. In: *Paper Conference and Trade Show PaperCon 2016*. Cincinnati, Ohio, USA, 15–18 May 2016. Peachtree Corners, Georgia, USA: TAPPI Press.
- Döll, H., 2010. Curtain coating – wenn der Forhang fällt. *Wochenblatt für Papierfabrikation*, 138(6), pp. 483–488.
- Kistler, S.F., 1983. *The fluid mechanics of curtain coating and related viscous surface flows with contact lines*. PhD thesis. University of Minnesota.
- Klass, C.P., 2004. Is curtain coating ready for prime time? *Solutions!*, 87(12), pp. 30–32.
- Lee, H.L., Youn, H.J., Lee, K.H., Kim, C.H. and Kim, J.D., 2009. Development of new coated linerboard by combining condebelt drying and curtain coating technologies. In: *63rd Appita Annual Conference and Exhibition*. Melbourne, 19–22 April 2009. Carlton, Vic.: Appita, pp. 203–210.
- Liu, C.Y., Vandre, E., Carvalho, M.S. and Kumar, S., 2016. Dynamic wetting failure and hydrodynamic assist in curtain coating. *Journal of Fluid Mechanics*, 808, pp. 290–315. <https://doi.org/10.1017/jfm.2016.594>.
- Marston, J.O., Hawkins, V., Decent, V.P. and Simmons, M.J.H., 2009. Influence of surfactant upon air entrainment hysteresis in curtain coating. *Experiments in Fluids*, 46(3), pp. 549–558. <https://doi.org/10.1007/s00348-008-0580-7>.
- Owens, D.K. and Wendt, R.C., 1969. Estimation of the surface free energy of polymers. *Journal of Applied Polymer Science*, 13, pp. 1741–1747. <https://doi.org/10.1002/app.1969.070130815>.
- Pekarovicova, A. and Fleming, III, P.D., 2005. *Innovations in ink on paper technology to improve printability*. Surrey, UK: Pira International.

- Renvall, S., Kumar, V., Toivakka, M. and Salminen, P., 2013. Short time water absorption into multilayer curtain coated linerboard. In: *Paper Conference and Trade Show (PaperCon 2013): Volume 1*. Atlanta, GA, USA, 27 April–1 May 2013. Peachtree Corners, GA, USA: Tappi Press, pp. 192–212.
- Schoenfelder, S.L., 2017. *The Modification of a curtain coating formulation: a study of rheology and surface tension, and their effect on pitting*. Master's Thesis. Western Michigan University.
- TAPPI, 2005. *T 701 pm-01 Gravimetric method for measuring dewatering of coating colors (Abo-Akademi-type method)*. Peachtree Corners, GA, USA: TAPPI.
- Triantafillopoulos, N., Grön, J., Luostarinen, I. and Paloviita, P., 2004. Operational issues in high-speed curtain coating of paper, Part 2: Curtain coating of lightweight coated paper. *TAPPI Journal*, 3(12), pp. 1–16.
- Tripathi, P., 2005. *Stabilization of curtain coater at high speeds*. PhD dissertation. Western Michigan University.
- Tripathi, P., Joyce, M., Fleming, P.D. and Sugihara, M., 2009. A statistical study of process variables to optimize a high speed curtain coater – Part I. *TAPPI Journal*, 8(1), pp 20–26.
- Urscheler, R., Dobler, F., Roper, J., Haavisto, J. and Nurmiainen, T., 2005. Key attributes and opportunities of multilayer curtain coating for paper. In: *TAPPI Coating Conference and Exhibit*. Toronto, Ontario, Canada, 17–20 April 2005. Norcross, GA, USA: TAPPI Press.

